SciMedCentral

Journal of Fractures and Sprains

Original Research

Taming Computational Irreducibility in Fracture Healing: A Physics-Informed AI Framework for the Shear-Shielding Nail-Plate Strategy

Chi-Ming Chiang[1,2]*

[1]*Center for General Education, Chung Yuan Christian University, China*
[2]*Department of Orthopedics, Yi-Her Hospital, China*

***Corresponding author**
Chi-Ming Chiang, Department of Orthopedics, Yi-Her Hospital, Center for General Education, Chung Yuan Christian University, China, Tel: 933216062

Submitted: 30 November 2025

Accepted: 22 December 2025

Published: 23 December 2025

ISSN: 2578-3831

Keywords
• Computational Irreducibility; Shear Shielding; Intramedullary Nailing; Augmentative Plating; Hypertrophic Nonunion; Mechanobiology; Interfragmentary Strain; Femoral Malrotation

Abstract

Background: Hypertrophic nonunion after intramedullary (IM) nailing represents a failed self-organization of the fracture healing system. In the language of Wolfram's principle of computational irreducibility, the coupled biological and mechanical cascade is a complex program whose exact trajectory cannot be shortcut. We identify the 'Shear Trap'—a localized dominance of transverse motion as the primary attractor state preventing self-organization.

Objective: To formulate a unified framework that links mechanoregulatory physics, interfragmentary strain (IFS) mathematics, and a physics-informed AI planner, and to illustrate its clinical application in femoral hypertrophic nonunion and shear-prone fractures treated with a shear-shielding nail-plate construct.

Methods: IFS was decomposed into axial (Δx) and transverse (Δy) components to quantify the "shear trap." Building on stiffness superposition, we modeled how adding a short non-locking 3.5-mm lateral plate in parallel to an IM nail alters the local strain field. A physics-informed surrogate model, trained on a library of finite-element simulations, was conceptualized to predict Δx and Δy for candidate nail-plate constructs and optimize plate length and position under constraints of osteogenic strain, cost, and implant availability. To validate this strategy, four femoral cases were treated with constructs adhering to vthese ector-control principles without nail exchange. The physics-informed AI planner serves as the computational proof-of-concept, defining the ideal mechanobiological boundaries (the 'Osteogenic Window'). The clinical series represents the empirical application of this shear-shielding heuristic in real-world scenarios.

Results: Theoretical modeling shows that nail-plate augmentation can move the construct from a shear-dominant regime (high Δy) toward an axial-favourable regime (preserved Δx with reduced Δy), consistent with mechanobiology favoring callus bridging. Clinically, three hypertrophic or shear-prone femoral cases achieved progressive consolidation after addition of a short lateral plate without nail exchange, with pain relief and functional recovery. In a fourth case, the same side-plating strategy was used to lock a corrected rotational alignment after symptomatic malrotation from IM nailing, with CT-confirmed restoration of near-symmetric femoral torsion.

Conclusion: By using AI to operationalize vector mechanics and shear control, the shear-shielding nail-plate construct suppresses the stochastic noise of transverse shear while preserving axial load sharing. This framework offers a mechanistically rational, cost-conscious, and potentially generalizable strategy to tame computational irreducibility in hypertrophic nonunion and shear-prone fractures.

INTRODUCTION

Fracture healing is a prototypical complex adaptive system in which local biomechanics (axial loading, shear, and torsion), inflammation, angiogenesis, and cell-fate decisions co-evolve across time. Contemporary mechanobiology emphasizes that not only the magnitude but also the directionality and timing of interfragmentary motion shape tissue differentiation, such that controlled axial micromotion can promote callus formation whereas excessive shear or torsion may disrupt bridging and perpetuate fibrous repair [1-4].

Hypertrophic nonunion after intramedullary (IM) nailing represents a mechanical phenotype in which biology is clearly active—evidenced by abundant callus—yet union fails. This paradox suggests that the local mechanical vector field remains unfavorable, commonly because transverse motion and rotation persist despite an apparently 'stable' construct [5,6]. This risk is amplified away from the femoral isthmus: in infra-isthmal/distal diaphyseal fractures, canal widening and a shorter distal segment reduce nail–bone coupling and allow greater bending and rotational micromotion, which are associated with delayed union and nonunion [7-9].

Orthopaedic dogma acts on scalars of stiffness, but biology responds to vectors ; strain directionality. Here, we argue that fracture healing is governed by vector mechanics: axial displacement (Δx) may be 'constructive' within a narrow window, whereas transverse displacement (Δy) and torsion act as 'disruptive noise' that prevents callus maturation and bridging. This framing provides a mechanistic rationale for augmentative lateral plating placed eccentrically relative to the nail—a shear-shielding adjunct that selectively suppresses shear and rotation while preserving axial load-sharing through the IM nail. Clinical and biomechanical evidence suggests that augmentative plating with the nail retained yields high union rates and superior rotational control compared with exchange nailing [10-12].

In this article, we integrate mechanobiological theory with the concept of computational irreducibility [13,14] to explain why small perturbations in construct geometry can lead to divergent healing trajectories that are difficult to predict analytically. We then propose a physics-informed AI planner that operationalizes directional mechanics into a low-cost decision aid for "shear-shielding" nail–plate augmentation, and we illustrate the framework with four cases: three hypertrophic or shear-prone femoral fractures treated by shear-shielding augmentation and one symptomatic rotational malalignment after IM nailing corrected using the same vector-control principle [15-21].

THEORETICAL FRAMEWORK: VECTOR MECHANICS OF SHEAR SHIELDING

Perren's interfragmentary strain theory expresses the mechanical stimulus at the gap as $\varepsilon = \Delta L/L$, where ΔL is the relative motion and L the initial gap length. Treating ΔL as a scalar, however, obscures the clinically relevant distinction between axial compression and transverse shear. To capture this, we decompose relative motion into axial (Δx) and transverse (Δy) components and define a vector-resolved IFS:

$$IFS \approx \sqrt{[(\Delta x)^2 + (\Delta y)^2]} / g,$$

where g is the effective gap length. Axial micromotion Δx is predominantly compressive and, within a moderate range of strain, is osteogenic and consistent with Wolff's law adaptation. Transverse shear Δy, by contrast, represents lateral sliding and bending-induced displacement at the near cortex. For a given total displacement, an increased Δy disproportionately elevates IFS and shifts tissue fate toward fibrous cartilage and delayed mineralization. The therapeutic goal of a shear-shielding construct is therefore to minimize Δy while keeping Δx within an osteogenic strain window [5,6].

An IM nail provides high axial stiffness k_x (resistance to shortening) but, especially in metaphyseal or oblique diaphyseal fractures with canal–nail mismatch, relatively low transverse stiffness k_t at the fracture plane. Under a shear force V, the transverse displacement at the gap can be approximated as $\Delta y \approx V/k_t$. In such configurations, Δy can be large despite apparently adequate "stiffness" in a scalar sense.

If a short, non-locking 3.5-mm lateral plate is added as an adjunct, it contributes an additional transverse stiffness k_p in parallel, such that the new transverse stiffness is $k_t' \approx k_t + k_p$ and the new transverse displacement becomes $\Delta y' \approx V/(k_t + k_p) < \Delta y$. Because the plate is eccentric to the neutral axis, it also acts as a buttress, shortening the effective shear lever arm at the near cortex and reducing local bending and rotational drift. Importantly, because the plate is short and non-locking, it does not transform the construct into an overly rigid bridging device; the IM nail continues to carry most of the axial load, allowing Δx to remain within an osteogenic range. The nail–plate frame is thus directionally rigid in shear and permissive in compression.

COMPUTATIONAL IRREDUCIBILITY AND THE PHYSICS-INFORMED AI PLANNER

Wolfram's principle of computational irreducibility states that many complex systems admit no closed-form shortcut: predicting their exact behaviour requires simulating the full dynamics. Fracture healing, with its nonlinear couplings between mechanics, vascularization, stem-cell recruitment, and matrix remodeling, fits this description. Even sophisticated mechanoregulatory and bioregulatory models cannot reliably predict, a priori, whether a given fracture in a particular patient will progress to union or stall in hypertrophic nonunion [13].

Work on coarse graining of cellular automata has refined this view by showing that, even when microscopic dynamics are irreducible, the macroscopic behaviour of a suitably coarse-grained system can become statistically predictable. We argue that hypertrophic nonunion after IM nailing is an instance of the system being trapped in an unfavourable micro-state space dominated by transverse shear. By selectively constraining the variable with the highest stochastic impact—Δy—we effectively perform a mechanical coarse-graining of the healing system. The nail–plate construct removes shear-driven randomness from the local mechanical field and forces the biology into a narrower, more predictable trajectory of endochondral ossification [14].

The physics-informed AI planner operationalizes this

conceptual framework by coupling mechanobiological constraints with resource constraints. Inputs can be obtained from standard preoperative imaging and clinical parameters, while the planner proposes a construct that preferentially reduces Δy and torsion without eliminating Δx. Such AI–biomechanics integration is increasingly recognized as a practical route to personalize orthopaedic decision-making, provided that physical constraints and transparent objectives are embedded into the model design [18–21] (Figure 1).

A physics-informed surrogate model is trained on a library of parametric finite-element simulations to approximate the mapping from design variables (e.g., plate length, eccentricity, and screw configuration) to mechanical outputs at the fracture site (Δx, Δy, and derived interfragmentary strain). In our proof-of-concept implementation, a set of 500 simulations was generated, after which the surrogate converged in approximately 2.5 hours on an NVIDIA A100 GPU, achieving ~98.2% predictive accuracy with a mean absolute error <0.05% strain for the output targets. This surrogate enables rapid exploration of the design space and real-time sensitivity to the shear component (Δy), which is computationally prohibitive with brute-force FE sweeps alone [18–20].

The surrogate and optimizer together generate model-based design–benefit curves (Figure 2), in which the predicted fraction of shear reduction is plotted against plate length for different eccentricities. These curves exhibit a characteristic saturation: most of the benefit is achieved with relatively short plates, especially when eccentricity is higher, whereas extending plate length beyond a certain point yields only marginal gains. This pattern motivates a "short-but-enough" philosophy for shear shielding, where the planner recommends the shortest plate that attains a desired reduction in Δy.

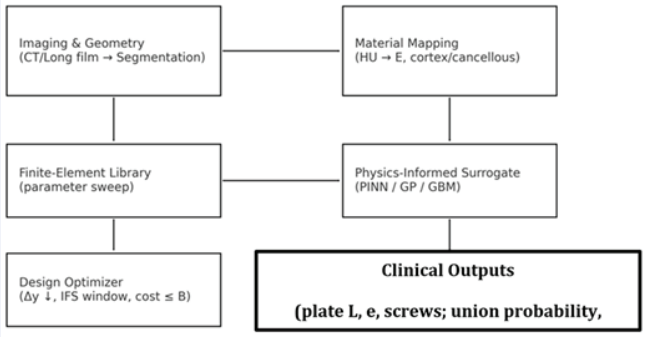

Figure 1 Workflow of the physics-informed AI planner for shear-shielding nail–plate constructs. Patient-specific imaging and geometry feed a finite-element library and material mapping; a physics-informed surrogate and design optimizer then generate clinically actionable construct recommendations.

Beyond internal mechanical metrics, the planner's clinical utility can be evaluated using decision-curve analysis (Figure 3). For a range of threshold probabilities of nonunion, we compare the net benefit of acting on the model against policies of adding a plate to every nailed fracture or never adding a plate. In an illustrative decision curve, the model-guided strategy provides greater net benefit across clinically relevant thresholds than either treat-all or treat-none strategies, suggesting that physics-informed AI guidance can improve patient-level decision-making once prospectively validated.

CLINICAL CASES

To demonstrate how the framework operates in

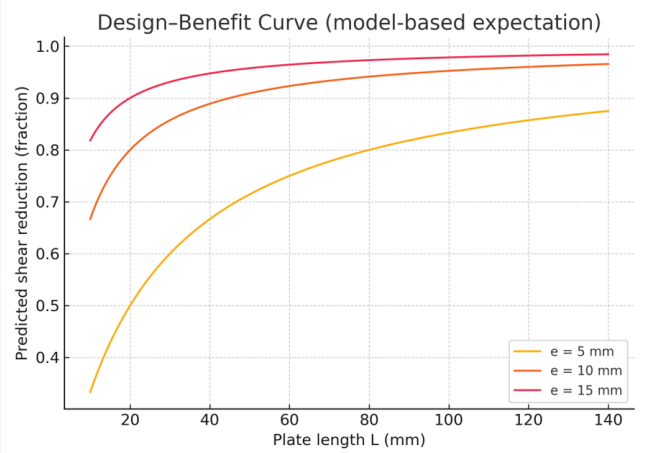

Figure 2 Model-based design–benefit curves for plate length and eccentricity. The predicted fraction of shear reduction at the fracture gap increases with plate length and eccentricity but exhibits diminishing returns, defining a minimum effective plate length.

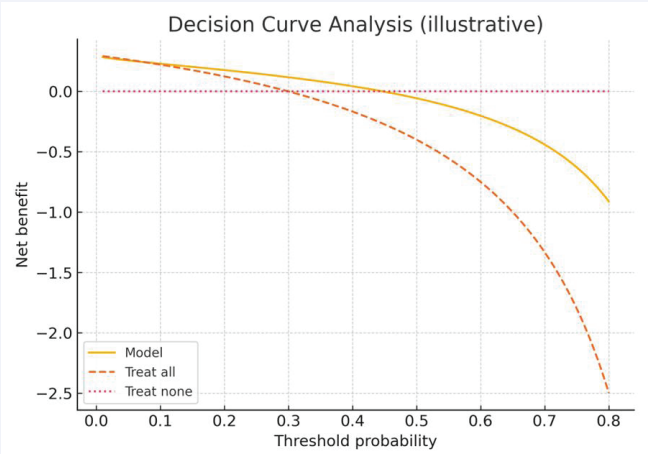

Figure 3 Illustrative decision-curve analysis for planner-guided shear shielding. Net clinical benefit for a model-guided strategy is compared with treat-all and treat-none policies across a range of threshold probabilities for nonunion.

real patients, we report four femoral cases in which a short lateral plate was added as a shear-shielding adjunct to an IM nail, without nail exchange. Clinical outcomes were followed longitudinally using pain scores (VAS), standardized radiographic healing scores where applicable (RUSH for proximal femur and RUST/mRUST for diaphyseal fractures), and objective imaging-based metrics for torsional alignment in the malrotation case (CT-based femoral torsion) [22–26].

Case 1 – Shear-prone proximal femoral nonunion after intramedullary nailing

A patient with a proximal femoral fracture initially underwent IM nailing. Alignment and length were restored, but the construct left a long oblique fracture line at the metaphyseal–diaphyseal junction with a relatively wide canal–nail mismatch. Clinically, the patient reported persistent pain and difficulty weight-bearing; radiographs demonstrated hypertrophic callus with an unbridged lateral cortex and subtle toggling of the proximal fragment, consistent with a shear-dominated gap environment.

Revision surgery consisted of adding a short non-locking 3.5-mm dynamic compression plate through a limited lateral approach, spanning the fracture with two bicortical screws per segment. No nail exchange was performed. The plate was positioned to neutralize shear and rotational drift rather than to create absolute compression. At follow-up, radiographs showed progressive bridging of the lateral cortex and maturation of callus, and the patient regained functional weight-bearing with pain relief (Figure 4). Post-operatively, the Radiographic Union Score for Hip (RUSH) improved to 10 at 6 months, and the Visual Analog Scale (VAS) for pain decreased from 8 pre-op to 1.

Case 2 – Post-polio femoral hypertrophic nonunion

A poliomyelitis-affected limb with long-standing muscular imbalance sustained a femoral shaft fracture. Initial fixation using a lateral plate with cerclage wiring failed; plate breakage occurred under cyclical loading with loss of alignment and progression to hypertrophic nonunion. Radiographs demonstrated exuberant callus but persistent lucency at the fracture site and mechanical instability.

Revision treatment consisted of inserting an IM nail to restore axial alignment and length, combined with a short non-locking lateral plate acting as an anti-shear buttress over the nonunion site. The plate was deliberately kept short, with a limited number of bicortical screws, to avoid converting the system into an overly rigid load-bearing construct. Following revision, the patient progressed to radiographic union with gradual consolidation of the fracture line and improved function (Figure 5). The RUST score progressed from 4 at revision to 11 at final follow-up.

Case 3 – Distal femoral metaphyseal fracture

Case 3 highlights a challenging mechanical zone: distal-third (infra-isthmal) diaphyseal/metaphyseal femoral fractures, where the medullary canal widens and the distal segment is short. Even with acceptable radiographic alignment, the nail–canal mismatch and proximity to the knee can permit disproportionate bending and rotational micromotion, predisposing to delayed union or nonunion [7–9]. A distal femoral fracture with an oblique, shear-prone geometry was initially treated with antegrade IM nailing. Despite adequate reduction, progressive hypertrophic callus with a persistent fracture line suggested ongoing shear at the metaphyseal interface.

Because antegrade nailing is most forgiving at the mid-shaft/isthmus, distal-third fractures have traditionally pushed surgeons toward retrograde nails or bulky distal femur plating. Here, we used the shear-shielding strategy to expand the usable envelope of antegrade nailing: a very short non-locking lateral plate was placed as a buttress to neutralize transverse shear and torsion at the distal segment while retaining axial load sharing through the nail. The construct progressed to consolidation without the morbidity of nail exchange or escalation to a long distal femur plate (Figure 6).

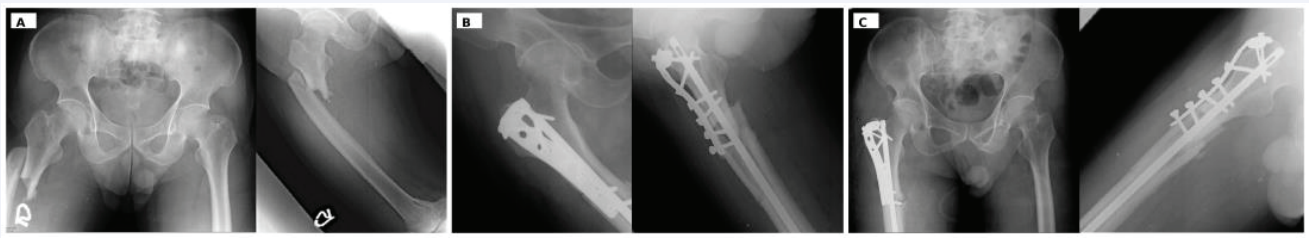

Figure 4 Case 1—shear-prone proximal femoral nonunion after intramedullary nailing. Pre- and post-augmentation radiographs illustrate how adding a short lateral plate converts a shear-dominated gap into a consolidating construct.

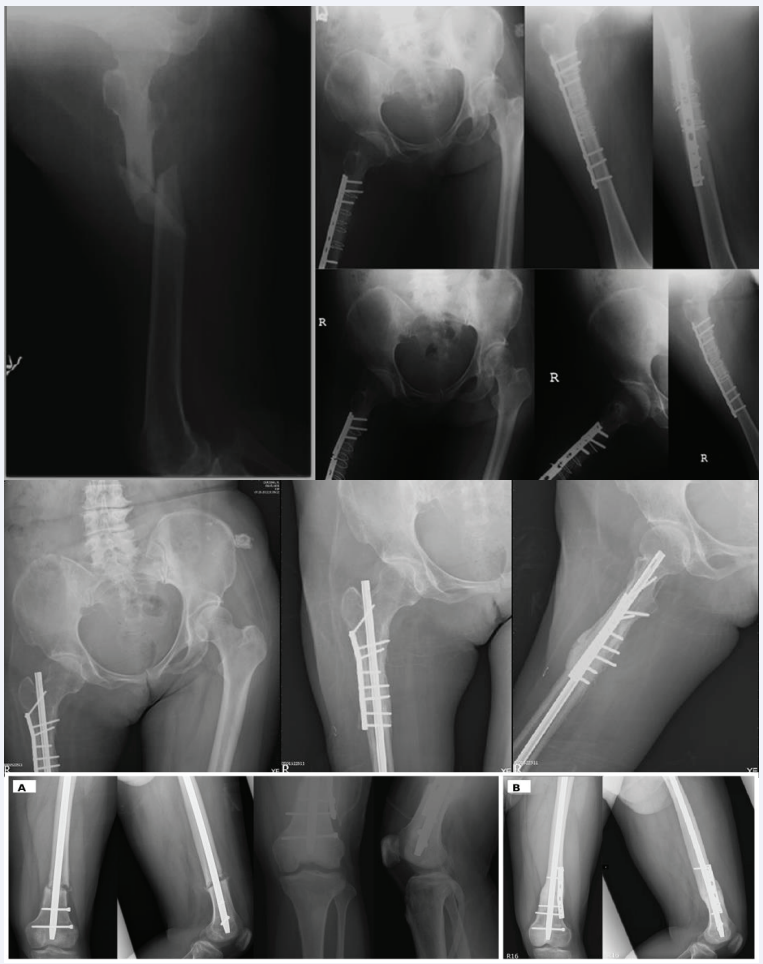

Figure 5 Vector-specific shear-shielding strategies in complex femoral phenotypes.
(Upper panel) Case 2: Post-polio hypertrophic nonunion. Standalone plating failed by fatigue fracture, consistent with persistent cyclic shear. Revision with an intramedullary nail plus a short lateral buttress plate preferentially reduced transverse motion (Δy) while preserving axial load sharing (Δx), enabling progressive consolidation.
(Lower panel) Case 3: Infra-isthmal distal femoral fracture. (A) Antegrade IM nailing in a distal-third, canal-widened segment with unfavorable nail–canal match, predisposed to bending/rotational micromotion. (B) Addition of a very short, non-locking lateral plate as a distal buttress to neutralize shear/torsion while maintaining axial dynamization, supporting consolidation on follow-up.

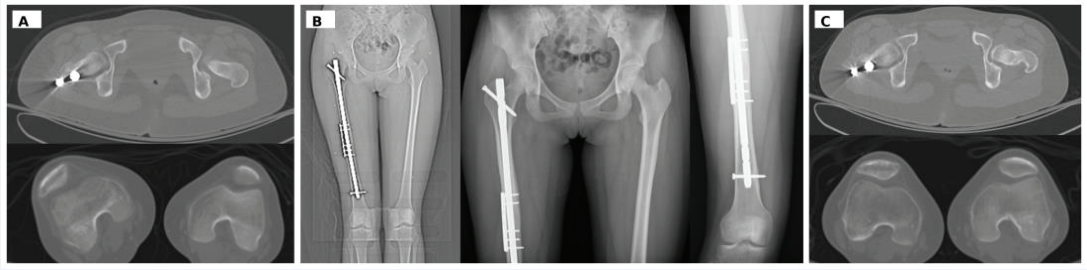

Figure 6 Vector-controlled correction of rotational instability (Case 4).Case 4—Correction of symptomatic rotational malalignment using a shear-shielding strategy.(A, B) Quantifying Torsional Noise: Axial CT images of the proximal and distal femur establish the rotational baseline, revealing significant asymmetry (external rotation) compared to the contralateral side.(C) Vector-Lock Intervention: Post-correction radiographs demonstrate the hybrid construct. The intramedullary nail is retained to maintain axial load-sharing (Δx), while a short lateral DCP plate is applied as a precise "anti-rotation brake." This configuration effectively neutralizes torsional shear and locks the corrected alignment without the morbidity of nail exchange.

Case 4 – Correction of symptomatic rotational malalignment after femoral IM nailing

The fourth case illustrates that the same nail–plate 'vector control' principle can be applied beyond nonunion treatment, specifically for torsional instability and malalignment. A 14-year-old female sustained a femoral shaft fracture from a motorcycle accident and underwent antegrade interlocking nailing at an outside hospital. After fracture pain improved, she developed a symptomatic out-toeing gait. Computed tomography torsion measurements demonstrated substantial external rotational malalignment: the injured femur measured 28° external rotation compared with 5° on the contralateral side (23° malrotation). At 16-month follow-up, CT confirmed near-symmetry of torsion (injured 7° vs contralateral 5°), and the patient's gait normalized

In summary, across these distinct clinical scenarios—ranging from nonunion to rotational instability—the addition of a shear-shielding plate consistently redirected the healing trajectory. This suggests a common underlying mechanobiological rule that can be visualized as a dynamical system.

At 16-month follow-up, CT confirmed near-symmetry of torsion (injured 7° vs contralateral 5°), and the patient's gait normalized.

DISCUSSION

This integrated theoretical and clinical series reframes hypertrophic nonunion and other 'failed' constructs as problems of directional mechanics rather than global stiffness alone1. To rigorously define this mechanism, we map the fracture mechanobiology as a dynamical system in a phase space portrait (Figure 7).In this visualization, hypertrophic nonunion is not merely a biological failure but a system trapped in a "Hypertrophic Attractor"—a high-shear zone where stochastic transverse noise (Δy) prevents the biological algorithm from converging to union. Standard exchange nailing often fails to escape this attractor because it addresses scalar stability without filtering directional noise. Conversely, the shear-shielding nail-plate construct acts as a vector-specific filter. As illustrated by the intervention trajectory in Figure 7, this strategy does not aim for absolute rigidity (the origin) but effectively steers the system state vertically out of the "Shear Trap" and into a "Pocket of Reducibility" (Osteogenic Window). Within this pocket, defined by minimized shear but preserved axial dynamization, the otherwise computationally irreducible healing process becomes

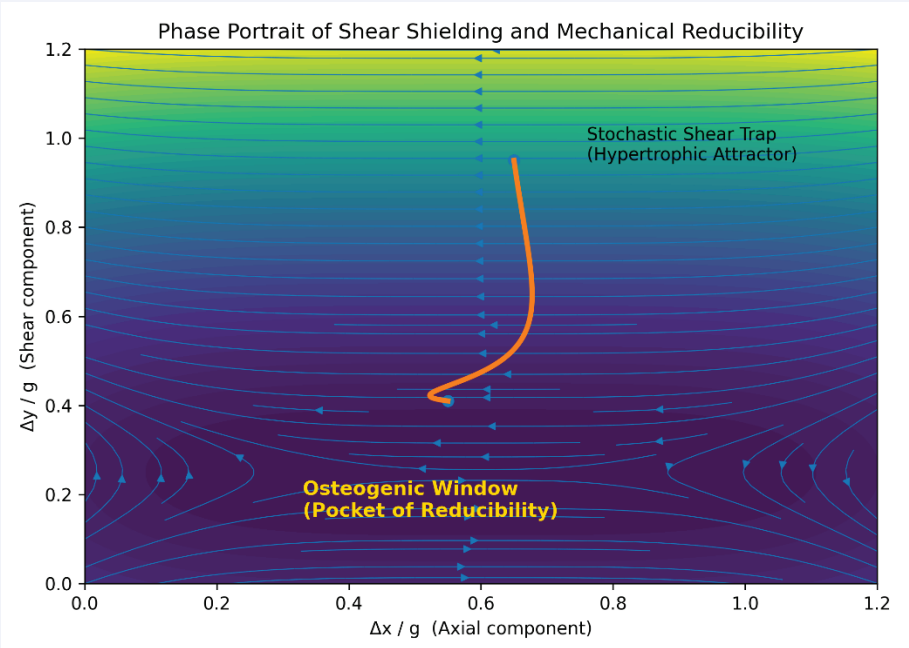

Figure 7 Visualizing the Mechanical Rescue Escaping the "Shear Trap." This phase portrait maps the fate of a fracture based on its movement patterns. (Top Area) The "Shear Trap" (High Shear, Δy): A chaotic zone where uncontrolled transverse motion prevents healing, leading to hypertrophic nonunion. (Bottom Area) The "Pocket of Reducibility" (Low Shear, Δy≈0): The safe zone where healing becomes biologically predictable. (Orange Path) The Intervention Trajectory: The nail-plate construct acts as a steering mechanism. It does not just make the construct "stiffer"; it selectively filters out the harmful shear, steering the fracture environment out of the chaotic trap and safely into the osteogenic pocket.

algorithmically predictable. The shear-shielding nail–plate construct selectively increases resistance to transverse displacement and rotation while maintaining axial load sharing, thereby modulating the mechanobiological signals that drive callus maturation [1–4]. Case 3 is particularly instructive because infra-isthmal/distal-third femoral fractures are mechanically disadvantaged for antegrade nailing due to canal widening and a shorter distal segment; radiographic studies identify these features as predictors of nonunion and emphasize the importance of distal fixation density [7–9]. Our approach extends the functional range of antegrade nailing into the distal third by adding a minimal, low-profile buttress that targets Δy and torsion. Case 4 further shows that the same vector-control logic can be leveraged to correct and stabilize rotational malalignment while preserving the original nail, avoiding more extensive revision constructs [15–17]. These observations align with broader clinical and biomechanical literature demonstrating that augmentative plating with the nail retained improves rotational stability and can outperform exchange nailing in femoral shaft nonunion [10–12].

The physics-informed AI planner provides a way to standardize and scale this reasoning. By training a surrogate model on parametric FE libraries, the planner can estimate how plate geometry and eccentricity tune Δx and Δy, and then optimize toward a 'safe' mechanobiological corridor under resource constraints [18–21]. Decision-curve analysis offers a clinically interpretable bridge between predicted mechanical benefit and the threshold probabilities at which a surgeon would choose augmentation, although the present work remains a conceptual demonstration that requires prospective validation.

Several limitations should be noted. This is a small case series without a control group, and heterogeneity in fracture pattern, biology, and follow-up precludes inference of comparative effectiveness. Nevertheless, the cases were documented with standardized pain reporting and objective radiographic/CT metrics, supporting the central thesis that directional control of interfragmentary motion can shift trajectories in systems that otherwise exhibit computational irreducibility [13,14]. Future work should prospectively couple serial union scores (e.g., RUST/mRUST or RUSH) with patient-reported outcomes and gait/rotation metrics, and should benchmark the AI planner against conventional decision-making in multi-center cohorts.

CONCLUSION

First, decomposing interfragmentary motion into axial (Δx) and transverse (Δy) components clarifies that transverse shear is the dominant mechanical driver of hypertrophic nonunion after IM nailing. The therapeutic target should be selective suppression of Δy rather than indiscriminate increases in global rigidity.

Second, a short, non-locking lateral plate added to an IM nail functions as a shear-shielding buttress that raises transverse stiffness ($k_t \rightarrow k_t' \approx k_t + k_p$), shortens the shear lever arm, and preserves beneficial axial micromotion. This rebalances the construct to be rigid in shear and flexible in compression, creating a mechanical "pocket of reducibility" within an otherwise computationally irreducible healing process.

Third, a physics-informed AI planner, grounded in mechanoregulatory principles and finite-element data, can prospectively identify shear-prone patterns and recommend the minimum effective dose of hardware. Future work should include patient-specific FE validation, radiostereometric measurements of early micromotion, and prospective trials comparing planner-guided constructs with standard care in terms of time-to-union, reoperation, and cost.

REFERENCES

1. Hast M, Glatt V, Archdeacon M, Ledet E, Lewis G, Ahn J, et al. Biomechanics of fracture healing: how best to optimize your construct in the OR. OTA Int. 2024; 7: e304.
2. Gläser N, Schröder M, Barcik J, Haffner-Luntzer M, Wehrle E. Extended view on the mechanobiology of fracture healing: interplay between mechanics and inflammation. Front Bioeng Biotechnol. 2025; 13: 1652897.
3. Bottlang M, Shetty SS, Blankenau C, Wilk J, Tsai S, Fitzpatrick DC, et al. Advances in Dynamization of Plate Fixation to Promote Natural Bone Healing. J Clin Med. 2024; 13: 2905.
4. Han Z. Axial micromotion locking plate construct can promote fracture healing. Front Bioeng Biotechnol. 2021.
5. Augat P, Burger J, Schorlemmer S, Henke T, Peraus M, Claes L. Shear movement at the fracture site delays healing in a diaphyseal fracture model. J Orthop Res. 2003; 21: 1011-1017.
6. Mavčič B, Antolič V. Optimal mechanical environment of the healing bone fracture/osteotomy. Int Orthop. 2012; 36: 689-695.
7. Watanabe Y, Takenaka N, Kobayashi M, Matsushita T. Infra-isthmal fracture is a risk factor for nonunion after femoral nailing: a case-control study. J Orthop Sci. 2013; 18: 76-80.
8. Kim JW, Oh CW, Oh JK, Park KH, Kim HJ, Kim TS, et al. Treatment of infra-isthmal femoral fracture with an intramedullary nail: Is retrograde nailing a better option than antegrade nailing? Arch Orthop Trauma Surg. 2018; 138: 1241-1247.
9. Hung WC, Hsu CJ, Kumar A, Tsai CH, Chang HW, Lin TL. Perioperative Radiographic Predictors of Non-Union in Infra-Isthmal Femoral Shaft Fractures after Antegrade Intramedullary Nailing: A Case-Control Study. J Clin Med. 2022; 11: 3664.
10. Jin YF, Xu HC, Shen ZH, Pan XK, Xie H. Comparing Augmentative

Plating and Exchange Nailing for the Treatment of Nonunion of Femoral Shaft Fracture after Intramedullary Nailing: A Meta-analysis. Orthop Surg. 2020; 12: 50-57.

11. Motififard M, Mousavi H, Iranpanah N, Akbari Aghdam H, Teimouri M, Aliakbari M, et al. Comparative Study of Exchange Nailing and Augmentative Plating for Treating Aseptic Nonunion of Femoral Shafts Post Intramedullary Nailing: A Single-Blind, Multicentric Randomized Clinical Trial. J Clin Med. 2024; 13: 6928.

12. Walcher MG, Day RE, Gesslein M, Bail HJ, Kuster MS. Augmentative Plating versus Exchange Intramedullary Nailing for the Treatment of Aseptic Non-Unions of the Femoral Shaft-A Biomechanical Study in a SawboneTM Model. J Pers Med. 2023; 13: 650.

13. Wolfram S. A New Kind of Science. Wolfram Media. 2002.

14. Israeli N, Goldenfeld N. Computational irreducibility and the predictability of complex physical systems. Phys Rev Lett. 2004; 92: 074105.

15. Jaarsma RL, Pakvis DF, Verdonschot N, Biert J, van Kampen A. Rotational malalignment after intramedullary nailing of femoral fractures. J Orthop Trauma. 2004; 18: 403-409.

16. Karaman O, Ayhan E, Kesmezacar H, Seker A, Unlu MC, Aydingoz O. Rotational malalignment after closed intramedullary nailing of femoral shaft fractures and its influence on daily life. Eur J Orthop Surg Traumatol. 2014; 24: 1243-1247.

17. Branca Vergano L, Coviello G, Monesi M. Rotational malalignment in femoral nailing: prevention, diagnosis and surgical correction. Acta Biomed. 2020; 91: e2020003.

18. Lewis GS, Mischler D, Wee H, Reid JS, Varga P. Finite Element Analysis of Fracture Fixation. Curr Osteoporos Rep. 2021; 19: 403-416.

19. Wee H, Reid JS, Chinchilli VM, Lewis GS. Finite Element-Derived Surrogate Models of Locked Plate Fracture Fixation Biomechanics. Ann Biomed Eng. 2017; 45: 668-680.

20. Kudela J, Matousek R. Recent advances and applications of surrogate models for finite element method computations: a review. Soft Comput. 2022: 26; 13709-13733.

21. Farhadi F, Barnes MR, Sugito HR, Sin JM, Henderson ER, Levy JJ. Applications of artificial intelligence in orthopaedic surgery. Front Med Technol. 2022; 4: 995526.

22. Frank T, Osterhoff G, Sprague S, Garibaldi A, Bhandari M, Slobogean GP; FAITH Investigators. The Radiographic Union Score for Hip (RUSH) Identifies Radiographic Nonunion of Femoral Neck Fractures. Clin Orthop Relat Res. 2016; 474: 1396-1404.

23. Panchoo P, Laubscher M, Held M, Maqungo S, Ferreira N, Simpson H, et al. Radiographic union score for tibia (RUST) scoring system in adult diaphyseal femoral fractures treated with intramedullary nailing: an assessment of interobserver and intraobserver reliability. Eur J Orthop Surg Traumatol. 2022; 32: 1555-1559.

24. Urva M, Challa ST, Haonga BT, Eliezer E, Working ZM, El Naga A, et al. Reliability of Modified Radiographic Union Score for Tibia Scores in the Evaluation of Femoral Shaft Fractures in a Low-resource Setting. J Am Acad Orthop Surg Glob Res Rev. 2022; 6: e21.00211.

25. Pavalko FM, Norvell SM, Burr DB, Turner CH, Duncan RL, Bidwell JP. A model for mechanotransduction in bone cells: the load-bearing mechanosomes. J Cell Biochem. 2003; 88: 104-112.

26. Saleh M, Royston S. Management of nonunion of fractures by distraction with correction of angulation and shortening. J Bone Joint Surg Br. 1996; 78: 105-109.